

INFLUENCE OF A VERTICAL MAGNETIC FIELD ON CONVECTION IN THE HORIZONTAL BRIDGMAN CRYSTAL GROWTH CONFIGURATION

L. Davoust,¹ R. Moreau,¹ R. Bolcato,¹
T. Alboussière,² A.C. Neubrand,² and J.P. Garandet²

This paper is a review of recent results on the MHD damping and reorganization of the convective flow present in the liquid pool of a horizontal Bridgman furnace during crystal growth. An asymptotic analysis, based on the assumption $Ha \gg 1$ and concerning the fully-established regime, predicts the distribution of velocity, electric potential, current density, and temperature within the core for any cross-section shape. Numerical results obtained for $0 \leq Ha \leq 100$ complement this asymptotic theory and show how the typical MHD flow organization with cores, Hartmann layers, and side layers, builds up as Ha increases. And an experiment, using mercury to model the liquid pool, and equipped with 55 thermocouples, allows us to check these predictions. It also complements the theory, namely on the stabilizing influence of the magnetic field and on the flow in the end regions.

1. Introduction

The application of a magnetic field is one of the ways to control the liquid motion in the vicinity of the solidification front during crystal growth experiments (an analysis of the influence of convection on the defects of the crystal may be found in [1]). This is particularly important in the horizontal Bridgman configuration where natural convection is necessary, present, and usually turbulent. This paper surveys recent results on the case where the magnetic field is vertical. It reviews a theoretical analysis of the established regime based on an asymptotic theory when the Hartmann number is very large and

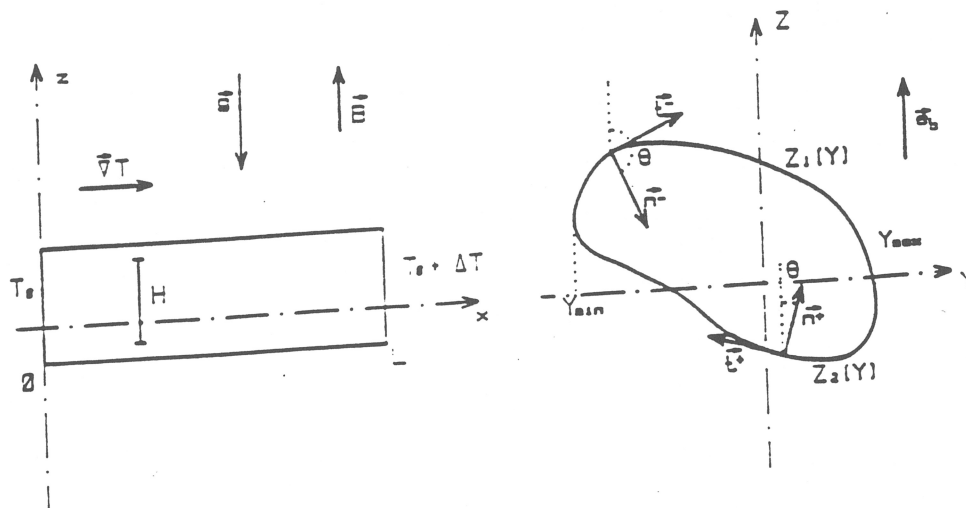


Fig. 1. Geometry and main notations ($X, Y, Z = x/H, y/H, z/H$).

¹INPG, Laboratoire MADYLAM, UA CNRS 1326, ENSHMG, BP 95, 38402 St Martin d'Hères Cedex, France.

²Commissariat à l'énergie atomique, DTA/CEREM/DEM/SES, CENG, 17 av. des Martyrs, 38054 Grenoble Cedex 9.

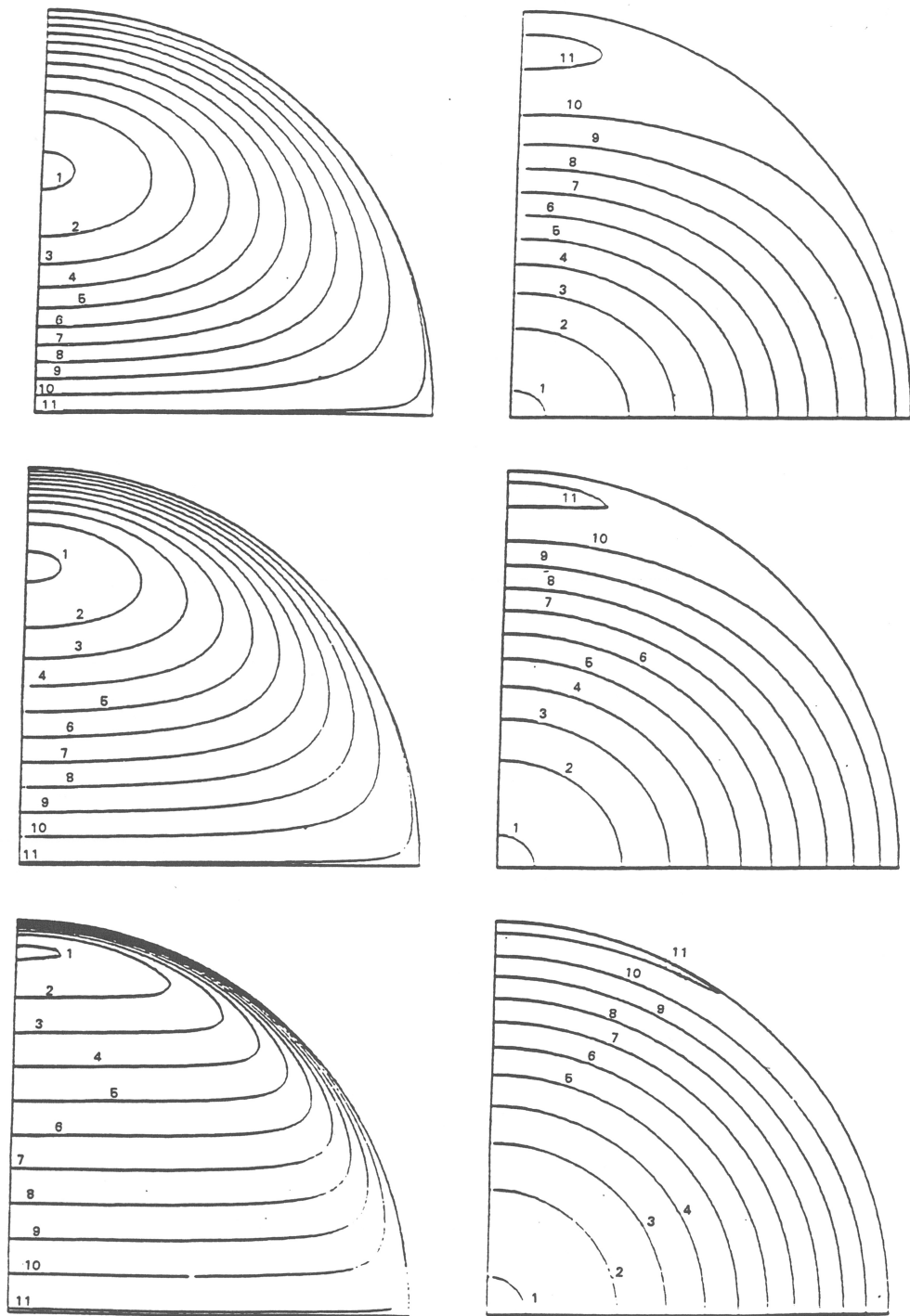


Fig. 2. Iso-velocity lines (left hand side) and electric current streamlines (right hand side) for $Ha = 5$ (top), 20 (middle), 100 (bottom) in the case of an electrically insulating circular wall.

on a numerical model when it is moderate. And it also presents some experimental data on the wall temperature distribution which is a quite significant image of the fluid flow.

2. Asymptotic Theory ($Ha \gg 1$)

The crucible is modeled as a horizontal cylinder of finite length L , whose cross-section has a typical length H (Fig. 1). The two ends are plane walls maintained at constant temperature T_1 and T_2 (T_1 is the melting temperature). The aspect ratio H/L is supposed small enough for a fully established regime to exist in the middle where the temperature distribution is

$$T = T_1 + GH [X + Pe \theta(Y, Z)]. \quad (1)$$

The Péclet number Pe is small enough to justify that, in a first approximation, the temperature in the middle part is proportional to X and the key parameter is the axial temperature gradient G , which is a priori unknown (G is only known in the limit of pure conduction: $G_0 = (T_2 - T_1)/L$). In non-dimensional form this parameter becomes a Grashoff number $Gr = \beta g GH^4/\nu^2$ (β is the expansion coefficient, g gravity, and ν kinematic viscosity). The applied magnetic field B_0 , which is the other control parameter, becomes, in non-dimensional form, the Hartmann number $Ha = (\sigma/\rho\nu)^{1/2} B_0 H$.

At high Hartmann number, the fully established regime has first been studied in the case of a two-dimensional cell (in the (x, z) plane) [2] and then a general theory has been developed for any cross-section shape defined by its upper and lower contour equations $Z_1(Y)$ and $Z_2(Y)$ [3]. Let us first limit ourselves to the case of a circular cylinder with an insulating wall. The non-dimensional axial velocity $U = uH/\nu$, current density $\mathbf{J} = \mathbf{j}H/B_0 \sigma\nu$, and electric potential $\varnothing = \varphi/B_0\nu$ have the following expressions within the core (index "c"):

$$U_c = -2(Gr/Ha^2)Z, \quad (2)$$

$$J_c = (Gr/Ha^2)[Ze_y - Ye_z], \quad (3)$$

$$\varnothing_c = (Gr/Ha^2)YZ. \quad (4)$$

It is noticeable that the electric current streamlines are circles and therefore close on themselves without passing through the Hartmann layer. This is an important property of such convective flows where the oddness of the velocity distribution [$U(-Z) = -U(Z)$] results in a zero net electric current through the core. This property makes the Hartmann layers electrically inactive, since they lose their key property in duct flows: to allow the closure of the electric current streamlines and thus to control the core velocity. The consequence is a very efficient braking of the convective flow as Ha^{-2} . By comparison, in duct flows this braking is as Ha^{-1} when the walls are insulating and as Ha^{-2} when the walls are electrically perfectly conducting. On the contrary, in this buoyant flow, the electrical conductance of the wall becomes almost irrelevant, since the core velocity is only half the value predicted by (2) if the wall is perfectly conducting.

An obvious consequence of the former results is that a rather moderate magnetic field might be capable of efficiently damping out convection and yielding quasi-diffusive conditions. This is clear for temperature whose disturbance due to convection is of the order of $Pe = Pr Gr/Ha^2$. With the low Prandtl number of liquid metals ($\approx 10^{-2}$) the requirement on Ha is easy to satisfy. However, to reduce the segregation due to the convective transport of chemical species whose diffusivity is very small ($D \approx 10^{-9} \text{ m}^2 \text{ s}^{-1}$), the requirement is more severe: $Pe_D < 1$, where $Pe_D = \nu/D Gr/Ha^2$, implies $Gr/Ha^2 < 10^{-2}$, which can still be satisfied on Earth with ordinary magnets but only at small or moderate scale H .

Let us now consider the case of a non-symmetric cross section such as half a cylinder [$Z_1 = 0, Z_2 = -(1/4 - Y^2)^{1/2}$]. Now, as shown in [3], the velocity distribution in the core becomes

$$U_c = (Gr/Ha^2) Z [(3^2\pi/2^8) \{((1/4) - Y^2)^{-1/2} + Y^2 ((1/4) - Y^2)^{-3/2}\} - (3/2)] \\ + (Gr/Ha)[(1/4)((1/4) - Y^2) - (3^2\pi/2^8)((1/4) - Y^2)^{1/2}], \quad (5)$$

and exhibits a new term proportional to Gr/Ha . This important consequence of the asymmetry is due to the fact that the J_y component of the current density within the core, of the order of Gr/Ha^2 , which now has a non-zero mean value, generates an opposite current through the Hartmann layers (if the wall is insulating), with a current density of the order of Gr/Ha . Now the Hartmann layers are electrically active and drive a core velocity of the same order of magnitude (Gr/Ha) just as in duct flows.

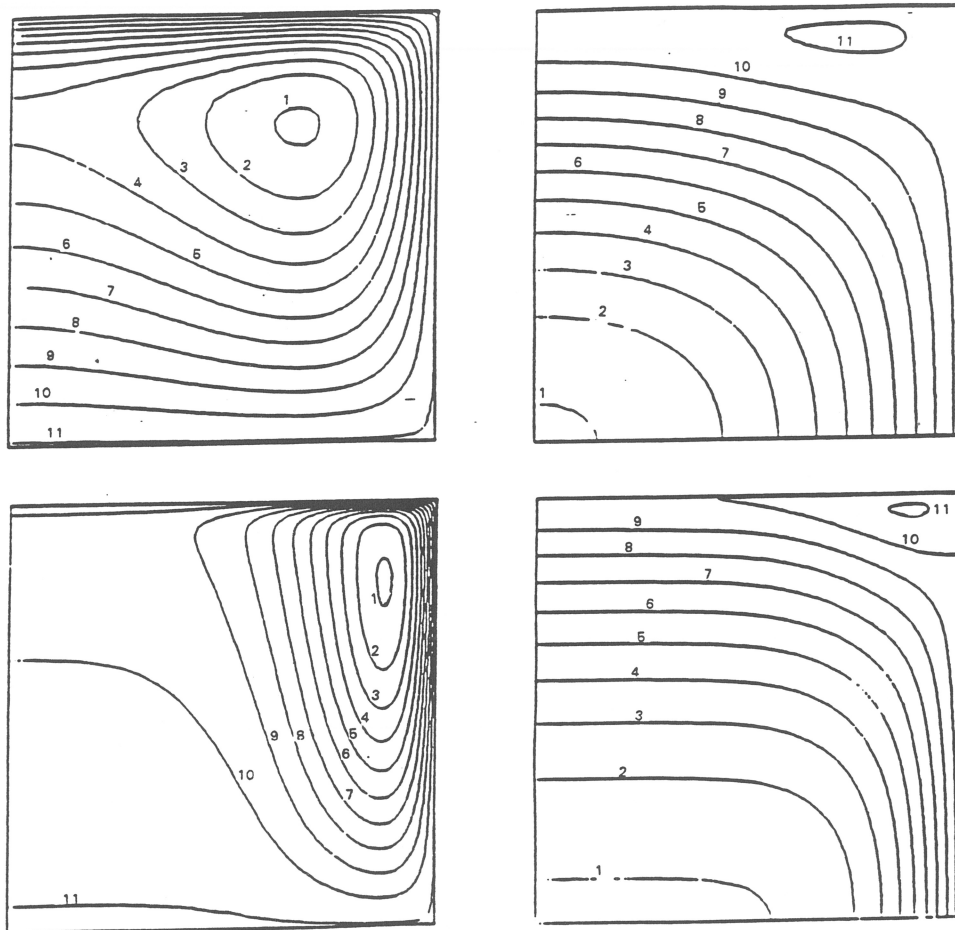


Fig. 3. Iso-velocity (left hand side) and electric current streamlines (right hand side) for $Ha = 20$ (top) and 100 (bottom), in the case of an electrically insulating square wall (only a quarter of the cross section is presented).

Quite recently, we were able to extend this theory to the case of weakly non-uniform magnetic fields of the form $B = B_0 + \lambda b$ with $\lambda \ll 1$ and $b \approx B_0$. It has been shown that, in some circumstances, the contribution of the non-uniform magnetic field to the core velocity scales as $\lambda Gr/Ha$, whereas the contribution of the uniform field scales as Gr/Ha^2 . These asymptotic results have a very important consequence. They demonstrate that the requirements on the geometry of the crucible and on the uniformity of the magnetic field are much more severe than what could be expected from an extrapolation of the scaling laws for symmetric crucibles and uniform magnetic fields.

3. Numerical Results

The former results, only valid for $Ha \gg 1$, have been completed with a numerical study based on the finite element code "Flux-Expert" [4] available in our laboratory. The non-dimensional velocity $U = uH/\nu$, induced magnetic field $B = b/B_0$, electric potential $\varnothing = \varphi/B\nu$, and temperature disturbance θ have been computed for different cross-section shapes (symmetric or not) and different values of the Hartmann number varying from zero to 10^2 . Because these quantities obey simple Poisson equations and classical Dirichlet or Neumann boundary conditions in the fully established regime, the numerics is straightforward and quite accurate. All comparisons with exact analytical results, such as the Birikh solution [5] for $Ha = 0$ or our asymptotic solution [3] for $Ha = 10^2$, confirm that the numerical results have a very good precision. Only a sample of these results is presented in Figs. 2 and 3 to illustrate the influence of the Hartmann number and the formation of the Hartmann layer (Figs. 2 and 3) and of the jet-like side layer (Fig. 3) in the case of the square cross section. In both cases, the way the electric current streamlines close on themselves, either within the core (circular section) or via the side

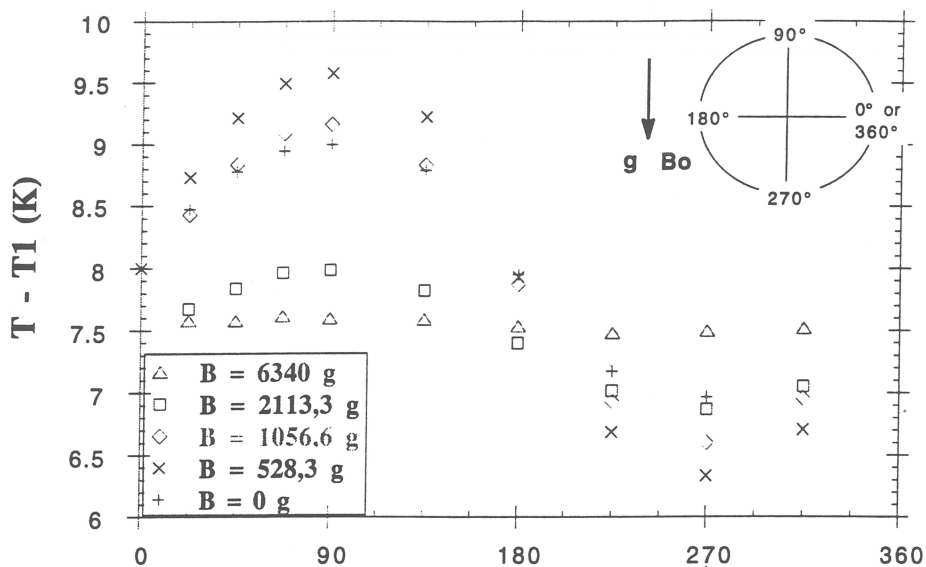


Fig. 4. Temperature distribution around the central circle for different values of the magnetic field ($T_0 = (T_1 + T_2)/2$).

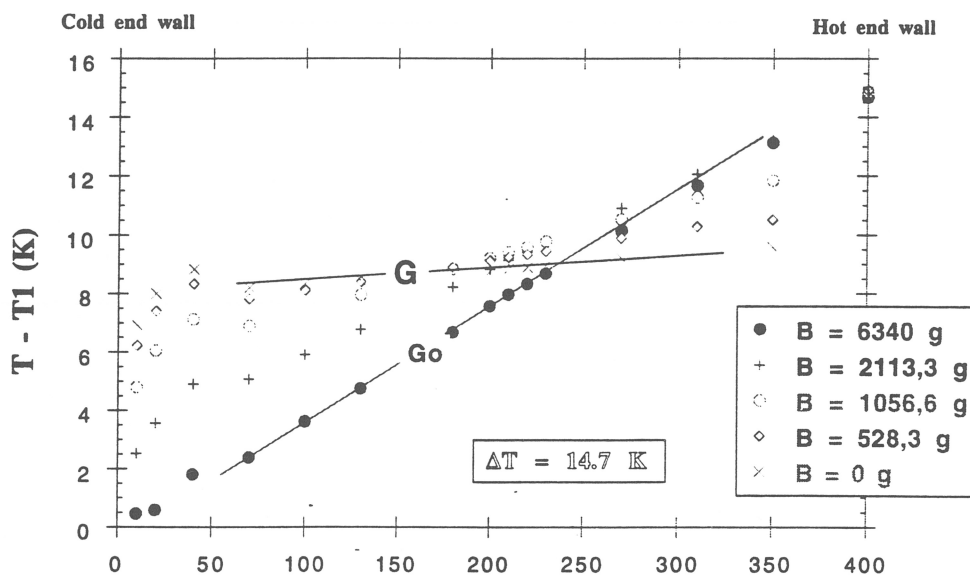


Fig. 5. Temperature distribution along the generatrix at 45° above the horizontal midplane, for different values of the magnetic field.

layers (square section) allows us to understand the velocity distribution. As in duct flows [6] the maximum velocity within the side layers is Ha times larger than the core velocity when $Ha \gg 1$.

4. Experimental Results

A mercury model (4 cm in diameter, 40 cm in length) has been realized. Two water cooled copper disks are installed at the ends of the cylinder and allow us to control their temperatures T_1 and T_2 at $\pm 2 \times 10^{-2}$ K. The wall is made of glass and is equipped with 55 thermocouples distributed on 11 circles (5 on each). A special device, containing a thermally insulating material and an external copper cylinder, is located around the glass tube and guarantees that, when the fluid is at rest, the temperature gradient within the mercury domain is uniform: $G_0 = (T_2 - T_1)/L$. The whole cell may be rotated around its horizontal axis in such a way that the sensors allow us to get the temperature at any point on a circle.

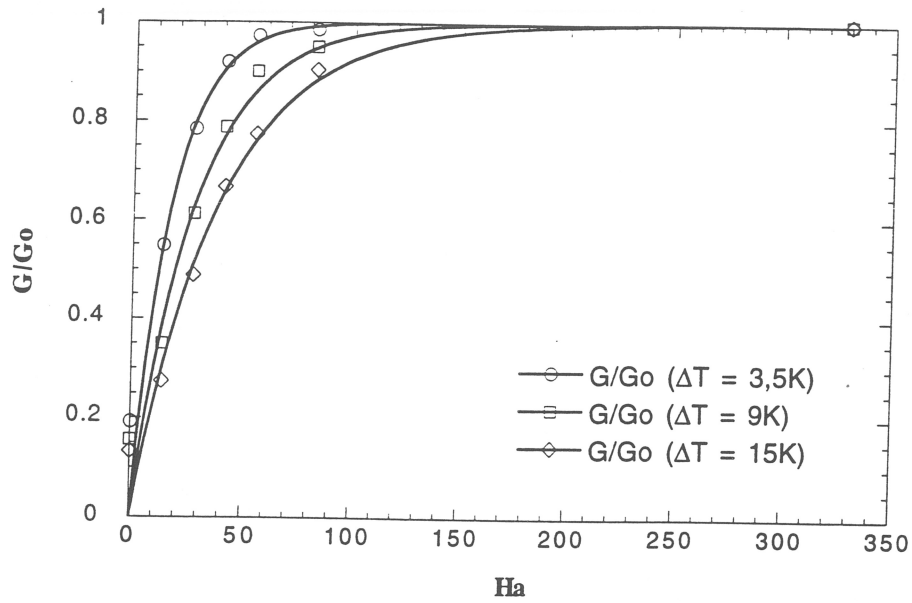


Fig. 6. Ratio between the actual axial temperature gradient G and its limit value G_0 in pure conduction versus Ha for different values of $T_2 - T_1$ (3.5 K, 9 K, 15 K).

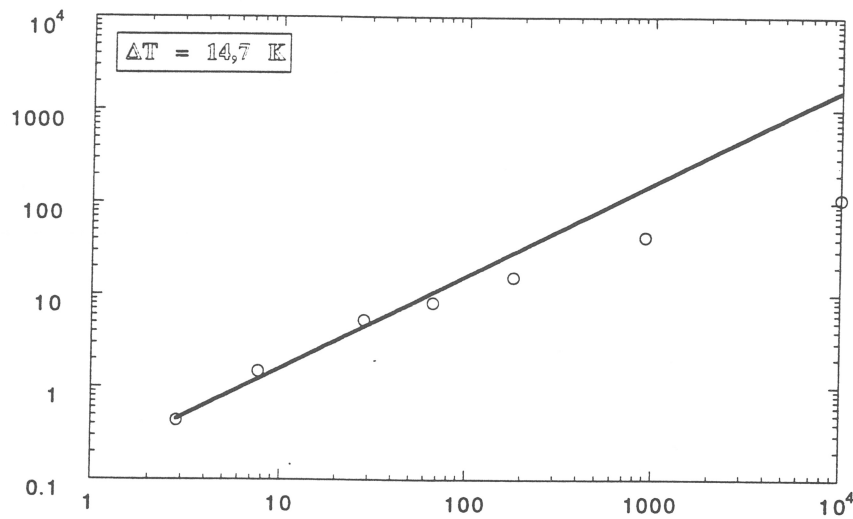


Fig. 7. Temperature jump $T_c - T_1$ versus Pe^2 (○: experimental data, —: $0.1583 Pe^2$).

Figures 4 and 5 show typical temperature distributions measured with $\Delta T = T_2 - T_1 = 14.7$ K. It is clear in Fig. 4 that the hot fluid travels near the top generatrix at 90° from the horizontal midplane and that the cold fluid travels near the bottom generatrix at 270° as expected. The experimental curves $T(\alpha)$ could easily be fitted with a sinusoidal function whose amplitude would give the maximum temperature variation within the cross section. Clearly, this amplitude increases first when B_0 increases from zero to 528 gauss (or $Ha \approx 27.5$), and then decreases to nearly zero when B_0 is 6240 G (or $Ha \approx 325$). This confirms the theoretical prediction that the convection can be reduced to a level low enough for having a temperature distribution controlled by conduction. The noticeable increase of the temperature disturbance when the magnetic field remains small will be explained later on. Similar temperature distributions have been recorded at different abscissa along the cylinder. In agreement with the predictions of the next speaker (Cowley [7]), when we get close enough to the cold end, a second order disturbance is superposed to this first order sinusoidal variation, which reveals a double-peaked profile. We interpret this second order disturbance as the signature of the three-dimensional descending end flow. This second order disturbance seems to be extremely sensitive to symmetry defects, so that the two peaks are rarely observed at exactly 45° and 135° .

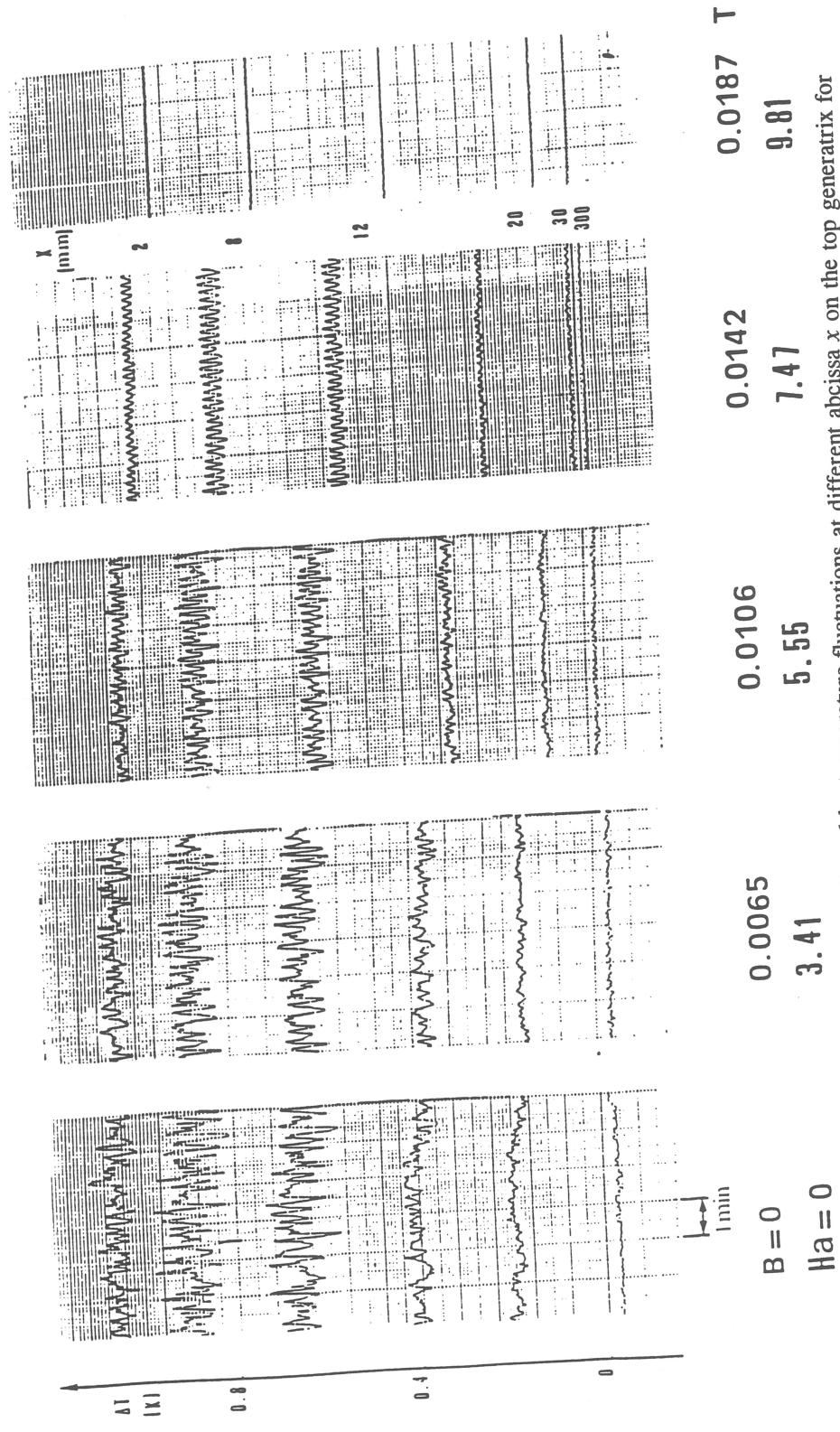


Fig. 8. Electromagnetic stabilization as indicated by temperature fluctuations at different abscissa x on the top generatrix for $T_2 - T_1 = 15$ K ($Gr \approx 3.3 \times 10^5$) and for different values of the Hartmann number.

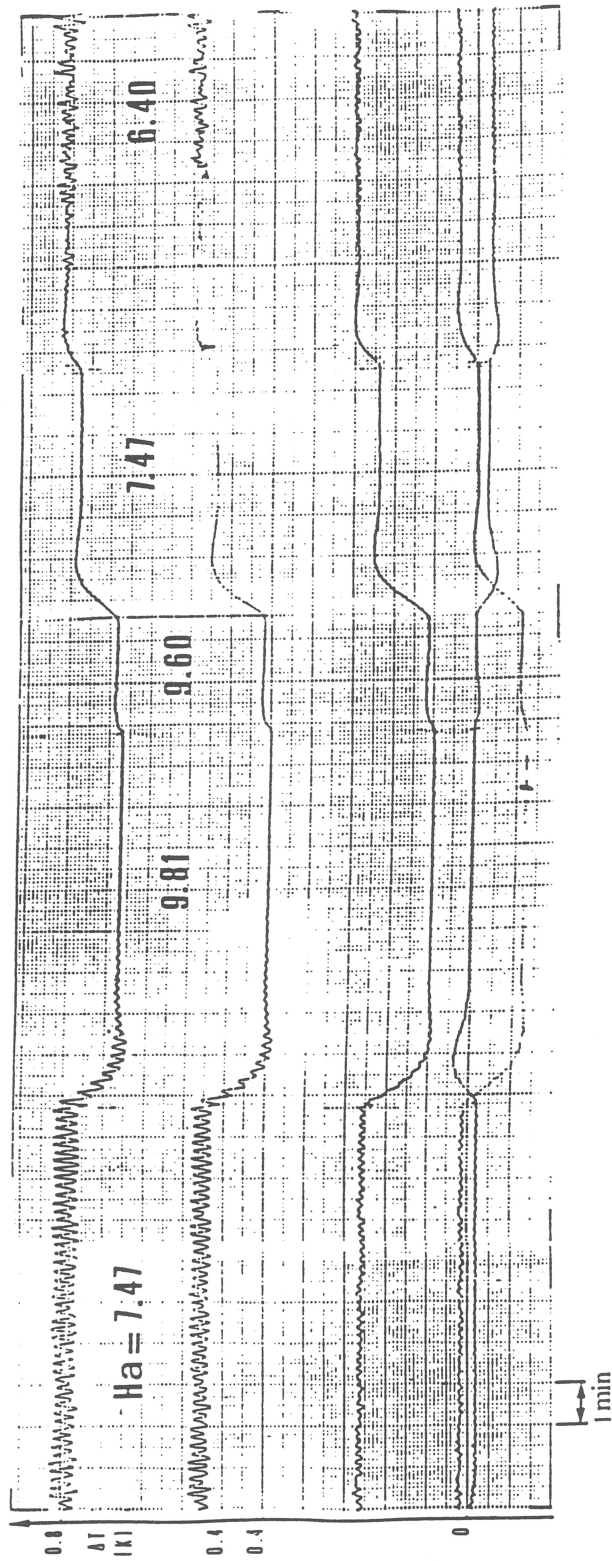


Fig. 9. Time evolution of the temperature disturbances when the magnetic field is suddenly changed, demonstrating some hysteresis and suggesting a subcritical bifurcation.

Figure 5 shows the x -dependence of the temperature on the generatrix located at 45° . The first feature to notice is the linear temperature gradient G in the middle part of the cell (except in end regions whose typical length is nearly two diameters), which varies significantly with the applied magnetic field (see Fig. 6). Indeed the value of G , or the ratio G/G_0 seems to be a good indicator of the convection level; from Fig. 6, we could conclude that, whatever the Grashoff number, a Hartmann number of the order of 150 is necessary to significantly reduce the difference between G and G_0 . Now, when the linear temperature variation observed in the middle is extrapolated until the cold end, a temperature jump may be deduced from the difference between this limit T_c and the end temperature T_1 . This jump, $T_0 - T_1$, which is a measure of the recirculating end flow, is plotted versus Pe^2 in Fig. 7. It seems clear that, when $Pe < 10$, the temperature jump follows a Pe^2 dependence. Again this confirms the theoretical predictions made by Cowley [7].

One of the most interesting experimental results is the apparently strong stabilization of the flow when the Hartmann number reaches values of the order of a few units, for a large Grashoff number ($Gr > 10^5$), as indicated by the temperature fluctuations (Figs. 8 and 9). It is clear that these fluctuations are completely damped out when $Ha = 9.8$. Although the level of fluctuation significantly varies with the abscissa (it is larger at 8 or 12 mm from the end than at 2 mm from the wall or at 20 mm or more), as it may be expected from the idea that the three-dimensional recirculation zone should be more unstable than the near-wall region or the fully established flow, it is clear that the transition takes place everywhere in the same time. It is also clear from Fig. 9 that the fluctuations disappear and appear at different values of the Hartmann number, depending on the way this control parameter is varied. From our first measurements, which still need to be completed and refined, it seems that, for $Gr 3.3 \times 10^5$ ($T_2 - T_1 = 15$ K), the critical Hartmann number is close to 9.8 when Ha is increasing and close to 7 when Ha is decreasing. This hysteresis suggests that the bifurcation is subcritical and that any stability analysis should be non-linear. This experimental study of the stabilization of this convective flow has still to be completed. In particular, it is our purpose to double this thermal diagnostic with an electric diagnostic, measuring the fluctuations of the induced electric potential as well as those of temperature. As a matter of fact, small eddies which have an associated Péclet number much smaller than one do not contribute to the temperature fluctuations (and escape to our first measurements) but contribute to the fluctuations of the electric potential.

This damping out of all fluctuations when Ha is larger than a few units certainly results in a suppression of the turbulence present at smaller Ha number and in a reduction of the effective viscosity (and diffusivities) to the molecular level. Then, in a first range of Ha values, while the electromagnetic braking remains small, the application of the magnetic field essentially results in a reduction of viscous friction. This could partially explain the increase of the temperature variation around the middle circle in Fig. 4. Another plausible explanation could be the suppression of cellular secondary flows as B increases [8].

5. Concluding Remarks

These studies on the influence of a vertical magnetic field demonstrate that it may be quite strong, even with moderate magnetic fields. When this field is increased from zero, the first effect to be observed is the apparent stabilization of the flow, as soon as Ha is above a critical value of the order of a few units. Then, when Ha reaches values of the order of a few tens, the fluid velocity becomes smaller and smaller. But the typical MHD organization of the velocity distribution with a core, Hartmann layers, and side layers (only for non-circular cells) requires higher values, above 10^2 , to be well established.

The temperature distribution itself, even though it is rather insensitive to the flow when the Péclet number is of order unity, is revealed to be significantly changed. The value of the axial temperature gradient G , which is proposed as an indicator of the convection intensity, may be strongly reduced by convection (from G_0 with a Hartmann number larger than 150 to nearly one tenth of G_0 without any magnetic field). As a consequence, the concentration of any chemical species, impurity or dopant, should be strongly dependent on the convection, and, therefore, strongly sensitive to an applied magnetic field. This would suggest that a vertical magnetic field might be an efficient tool to reduce and control segregation and other defects in horizontal Bridgman crystal growth. As shown in another paper (Alboussi re et al. [9]), our first results on segregation, which have been obtained with an axial magnetic field, also indicate that the axial field needs to be large to have a significant effect.

REFERENCES

1. W. E. Langlois, "Buoyancy driven flows in crystal growth melts," *Ann. Rev. Fluid Mech.*, **17**, 191-215 (1985).
2. J. P. Garandet, T. Alboussière, and R. Moreau, "Buoyancy driven convection in a rectangular enclosure with a transverse magnetic field," *Int. J. Heat Mass Trans.*, **35**, 741-748 (1992).
3. T. Alboussière, J. P. Garandet, and R. Moreau, "Buoyancy driven convection with a uniform magnetic field. Part I. Asymptotic analysis," *J. Fluid Mech.*, **253**, 545-563 (1993).
4. Ph. Massé, "Modeling of continuous media methodology and CAD of finite element program," *Intermag Conf.*, Hamburg, FRG, 1984.
5. R. V. Birikh, "Thermocapillary convection in a horizontal layer of liquid," *J. Applied Mech. Tech. Phys.*, **3**, 69-72 (1966).
6. J. C. R. Hunt, "Magnetohydrodynamic flow in rectangular ducts," *J. Fluid Mech.*, **21**, 577-590 (1965).
7. M. D. Cowley, "On the temperature distribution due to convection in the horizontal Bridgman crystal-growth configuration with vertical magnetic field," *2nd Int. Conf. on Energy transfer in MHD flows*, Aussois, France, 1994.
8. H. Ben Haddid, and D. Henry, Private communication, 1994.
9. T. Alboussière, A. C. Neubrand, J. P. Garandet, and R. Moreau, "Magnetic field and segregation during Bridgman growth," *2nd Int. Conf. on Energy transfer in MHD Flows*, Aussois, France, 1994.